Journal of Applied Polymer Science

Functionally Modified, Melt-Electrospun Thermoplastic Polyurethane Mats for Wound-Dressing Applications

Christoph Hacker,[1] Zeynep Karahaliloglu,[2] Gunnar Seide,[1] Emir Baki Denkbas,[2,3] Thomas Gries[1]

[1]Institut fuer Textiltechnik, Rheinisch-Westfaelische Technische Hochschule, Aachen 52074, Germany

[2]Nanotechnology and Nanomedicine Division, Hacettepe University, Beytepe 06800, Ankara, Turkey

[3]Biochemistry Division, Department of Chemistry, Hacettepe University, Beytepe 06800, Ankara, Turkey

Correspondence to: C. Hacker (E-mail: christoph.hacker@ita.rwth-aachen.de)

ABSTRACT: The electrospinning of a polymer melt is an interesting process for medical applications because it eliminates the cytotoxic effects of solvents in the electrospinning solution. Wound dressings made from thermoplastic polyurethane (TPU), particularly as a porous structured electrospun membrane, are currently the focus of scientific and commercial interest. In this study, we developed a functionalized fibrillar structure as a novel antibacterial wound-dressing material with the melt-electrospinning of TPU. The surface of the fibers was modified with poly(ethylene glycol) (PEG) and silver nanoparticles (nAg's) to improve their wettability and antimicrobial properties. TPU was processed into a porous, fibrous network of beadless fibers in the micrometer range (4.89 ± 0.94 μm). The X-ray photoelectron spectroscopy results and scanning electron microscopy images confirmed the successful incorporation of nAg's onto the surface of the fiber structure. An antibacterial test indicated that the PEG-modified nAg-loaded TPU melt-electrospun structure had excellent antibacterial effects against both a Gram-positive *Staphylococcus aureus* strain and Gram-negative *Escherichia coli* compared to unmodified and PEG-modified TPU fiber mats. Moreover, modification with nAg's and PEG increased the water-absorption ability in comparison to unmodified TPU. The cell viability and proliferation on the unmodified and modified TPU fiber mats were investigated with a mouse fibroblast cell line (L929). The results demonstrate that the PEG-modified nAg-loaded TPU mats had no cytotoxic effect on the fibroblast cells. Therefore, the melt-electrospun TPU fiber mats modified with PEG and nAg have the potential to be used as antibacterial, humidity-managing wound dressings. © 2013 Wiley Periodicals, Inc. J. Appl. Polym. Sci. **2014**, *131*, 40132.

KEYWORDS: biocompatibility; electrospinning; functionalization of polymers; polyurethanes

Received 8 May 2013; accepted 27 October 2013

DOI: 10.1002/app.40132

INTRODUCTION

An ideal wound dressing should consist of a number of key attributes, including the ability to absorb the exudates of the wound, to provide a moist environment for the wound, and to prevent an entry for microorganisms into the wound. In addition, it has to show mechanical resistance and hemostatic ability.[1,2]

Polyurethane (PU) is a thermoset and thermoplastic polymer. It is an attractive material in biomedical applications because of its advanced elastomechanical and biological properties. Thermoplastic polyurethane (TPU) materials are often used as films or foams in wound-dressing applications because of their unique properties, including their blood compatibility, air permeability, and well-supported barrier.[3–6] PU-based wound-dressing materials, such as Tegaderm and OpSite, are commercial products on the market.[3,7] Tegaderm and OpSite are semipermeable film-type wound dressings. This type of wound dressing absorbs only a limited amount of exudate because of its compact structure. Foam-type dressings can cause bacterial contamination, which delays the healing process.[8] Hence, the development of an antibacterial wound-dressing material with an open porous structure is still an issue.

For bacteria, a wound is a primary entry point because of its favorable environmental conditions, which include moisture and a warm and nutrient-rich medium. On the basis of this, a wound dressing has to prevent microorganism growth around the wound area, for example, with an antibacterial functionalization. In the past few years, dressing materials, including silver or metallic compounds, have been in demand because of their strong antibacterial properties. The metal particles are added to the polymer, either in advance of electrospinning or after this process, by the coating of the surface of the polymer.[9,10] It has been reported that ionic silver (Ag^+) is effective against a broad range of microorganisms. Additionally, silver-coated dressings cause less irritation than silver nitrate solutions.[11] PU-foam-

and film-based antibacterial wound dressings are commercially available (Allevyn Ag, Acticoat Ag, and Polymem Silver). Allevyn Ag is a foam-film-based wound dressing containing silver sulfadiazine. Acticoat Ag and Polymem Silver include nanocrystalline particles. Silver nanoparticles (nAg's) are a preferred antibacterial agent because of their broad spectrum of antibacterial activity, for example, against Gram-positive and Gram-negative microorganisms[12] and antibiotic resistant bacteria, such as methicillin-resistant *Staphylococcus aureus*.[13] The investigations on nAg's in wound-dressing applications imply that a wound dressing containing these particles displays a controlled and prolonged silver release.[14] Additionally, *in vitro* and *in vivo* studies suggest that nAg's play an active role in wound healing by decreasing inflammation and scar formation.[15]

Electrospun fibers have advantages, including a higher surface-to-volume ratio and higher porosity compared to films, foams, and conventional nonwoven fabrication techniques.[16–18] Melt-electrospinning has attracted interest for medical applications. However, this research field still has still shown few experimental results in the literature.[19,20] Melt-electrospinning has many advantages in comparison to electrospinning from solution. It prevents the toxicity, preprocessing, and postprocessing due to the solvent usage. Therefore, no cytotoxic effects are expected, the production costs of the materials decrease, and environmental problems are prevented. Additionally, because of the simple process directly from the granule to the fiber, the material can be easily transformed into commercial products on an industrial scale.[19,21]

The aim of this study was to fabricate melt-electrospun, porous TPU mats and to evaluate the effect of surface modifications on the wettability, antibacterial activity, and cell viability. A poly (ethylene glycol) (PEG)-based plasma treatment of the TPU mats was used to modify the surface properties of the fibers. Subsequently, nAg's were incorporated into the PEG-modified TPU mats as antibacterial functionalization. The structure morphology, mechanical stability, and water-uptake and surface properties of the produced material were studied. Antimicrobial activity and cytotoxicity tests were conducted to highlight the potential use of these melt-electrospun mats for wound healing.

EXPERIMENTAL

Materials

The PU elastomer granulate, Elastollan 1185A (polyether type PU elastomer), was provided by BASF GmbH (Germany). Silver nitrate ($AgNO_3$), PEG ($M_w = 300$ Da), and phosphate-buffered saline (PBS; 0.1*M*, pH 7.4) were obtained from Sigma-Aldrich. Dulbecco's modified Eagle's medium, fetal bovine serum, penicillin–streptomycin, L-glutamine, and trypsin–ethylene diamine tetraacetic acid were purchased from Biological Industries (Israel). *S. aureus* (ATCC 25923) and *Escherichia coli* (ATCC 25922) were obtained from the American Type Culture Collection (Rockville, MD). Mueller Hinton Agar, nutrient broth, and Luria–Bertani medium were purchased from Merck (Germany). Mouse fibroblast cells (L929) were purchased from the American Type Culture Collection.

Melt-Electrospinning

The experimental setup included a high-voltage supply (Eltex KNH65, Eltex-Elektrostatik-GmbH, Weil am Rhein, Germany),

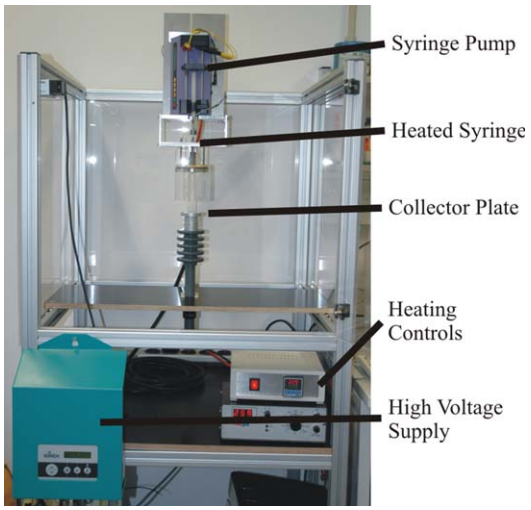

Figure 1. Image of the melt-electrospinning setup. [Color figure can be viewed in the online issue, which is available at wileyonlinelibrary.com.]

a digitally controlled syringe pump (11 Plus, Harvard Apparatus, Holliston) and two adjustable, custom-made heating devices for the polymer melt reservoir and nozzle (Figure 1). The polymer was molten within a glass syringe surrounded by a circular heating coil; a controlled flow rate was obtained with a plastic piston connecting the pump to the back of the syringe. A heated plate around the metallic nozzle served as a second heating zone. The thermocouple and hot-coil temperature were adjustable up to 400°C. The plate collector (from aluminum, diameter = 7 cm) was connected to the high-voltage supply.

To determine a stable spinning process, the voltage, the distance between nozzle and collector, the flow rate, and the temperatures were adjusted systematically. A stable spinning process was defined by a continuous jet from the Taylor Cone at the nozzle for the duration of approximately 2 min. Subsequently, the spun fibrous mat was removed along with the aluminum foil from the collector.

Characterization

The morphology and fiber diameter of the pure TPU mats and nAg-containing PU fiber structures were determined with scanning electron microscopy (SEM; JEOL, JSM7000F). For further examination of the nonwoven structure, the samples were immersed in liquid nitrogen for 10 min and then cut along their cross section with a sharp blade (sample thickness = 0.8 mm). The TPU samples were coated with gold with a sputter coater at 15 kV for 5 min. The TPU fiber diameters were measured with image processing software (ImageJ, NIST).

To demonstrate the application of the functional modification, the surfaces of the modified TPU samples with PEG and nAg were characterized with X-ray photoelectron spectroscopy (XPS; Thermo Scientific K-Alpha) to determine the elemental composition. The X-ray source was a monochromatized Al Kα X-ray (1486,6 eV). The pass energy of the analyzer was 50 eV for high-resolution core level spectra, and the beam spot was 400 μm. Elemental atomic percentages were measured with Thermo Avantage v4.41 software.

Thermal and Mechanical Properties

The glass-transition temperature (T_g) and melting temperature (T_m) of the pure polymer and fiber mat structure were determined with differential scanning calorimetry (DSC; DSC-1, Mettler-Toledo GmbH, Giessen, Germany) to evaluate the melt-electrospinning process effects on the thermal properties. The melt-electrospun fibers and pure polymer were heated between 25 and 250°C at 10°C/min under a nitrogen atmosphere.

The weight loss rate in relation to the temperature was determined by thermogravimetric analysis (TGA; TGA/DSC-1, Mettler-Toledo GmbH, Giessen, Germany) to indicate potential thermal decomposition due to the melt-electrospinning process. All of the measurements were conducted between room temperature and 800°C under a nitrogen atmosphere at a heating rate of 10°C/min

For a qualitative comparison of the mechanical properties (tensile strength and elongation) of the melt-electrospun TPU mats in dry and wet environments, samples were measured with a tensile testing machine (Zwick Roell Z 2.5 MA 18-1-3/7, Ulm, Germany). Because wound dressings are usually applied in a moist or wet environment, the mechanical properties should be maintained under humidity. For the analysis, the specimens were cut into dimensions of 1.5 × 0.5 × 0.08 cm^3 (Length × Width × Thickness). For the wet-state mechanical properties, TPU mats were placed in distilled water for 24 h at 25°C. All of the measurements were obtained under a crosshead speed of 10 mm/min with a 10-N load cell. Each sample was measured three times ($n = 3$).

Surface Modifications

To improve the capability of the TPU mat to absorb liquids, for example, wound exudate, a modification via PEG monomers was conducted. The surface properties of the TPU fiber mats were modified by treatment in a radio-frequency glow-discharge plasma deposition. The radio-frequency glow-discharge plasma deposition system (Vacuum Praha, Prague, Czech Republic) included a 13.56-MHz radio-frequency generator, vacuum reaction chamber, and vacuum pump. Samples were placed individually in a vacuum chamber between two electrodes. The chamber was flushed with argon gas three times to ensure that there were no stray reactive molecules. The system was then fed with the monomer (PEG), and glow discharge was created at a power of 35 W and 0.12 mbar. The samples were kept in the vacuum chamber for 20 min. Finally, the reaction chamber was cleaned with argon gas to remove any remaining reactive gas.

Subsequently, antibacterial modification was conducted. After the surface of the melt-electrospun TPU mats were modified with PEG, the TPU mats were immersed into 0.5 and 1 mg/mL $AgNO_3$ solutions, shaken overnight, and dried at room temperature. The mats were irradiated under a UV lamp (UV-A, $\lambda = 350$–400 nm). In this way, the Ag^+ ions were converted into nAg's. Before further tests, the nAg-loaded TPU mats were washed with distilled water.

Contact Angle and Water Uptake

We tested the capability of the mats to absorb liquids by testing the short-term wettability and long-term water uptake of the TPU mats. The water wettability of the modified and unmodified TPU surfaces was examined with a contact angle instrument (DSA100, KRUSS, Germany) at room temperature. Melt-electrospun samples were cut into dimensions of 0.5 × 0.5 cm^2 (Length × Width) for the analysis. According to the shape of drop, the contact angles were determined by the instrument's software. We calculated the average contact angle by measuring at different points (four points for each sample) on the same sample. Each measurement was performed in triplicate, and the standard deviation was calculated from these.

Melt-electrospun fiber mats were cut into uniform size (0.5 × 0.5 cm^2) to study the water-uptake behavior, and all of the water was removed from the mats by lyophilization (Martin Christ Alpha 2–4 LSC, Germany). The dried samples were weighed and immersed in distilled water at room temperature for 1 and 24 h. The samples were taken out of the water solution, excess surface water was removed with a filter paper, and the weight of the fiber mats was measured. The ability to take up water was calculated as follows. W_0 and W represent the initial and final weights of the TPU mat, respectively:

$$\text{Water uptake } (\%) = [(W - W_0)/W_0] \times 100$$

Silver Release

The silver release of the TPU mats is essential for antibacterial function. To evaluate the silver-release properties, particularly with respect to the amount of silver loading, melt-electrospun TPU mats were analyzed with inductively coupled plasma mass spectroscopy (ICP-MS; Thermo-Fisher). The samples (0.5 and 0.1 mg/mL nAg loaded melt-electrospun mats) were immersed into a tube containing 16 mL of deionized water and incubated at 37°C in a shaking incubator for 5 days. At the end of each day, 3 mL of solution was collected from the sample tube for analysis. Fresh deionized water was added to the sample tubes as intake volume. The samples were diluted 100-fold before ICP-MS analysis. Each sample was measured three times.

Antibacterial Study

To evaluate the antimicrobial properties of the nAg-loaded melt-electrospun TPU mats, they were tested by a disc-diffusion method. For the zone inhibition test, *S. aureus* was grown in nutrient broth, and *E. coli* was grown in Luria–Bertani medium overnight at 37°C at 250 rpm in shaking incubator. Each sample was cut into a disk shape (diameter = 0.5 cm) and then immersed in a 70% ethanol solution and sterilized. After the bacterial population was efficiently increased, saline solution was added to the cultured organism solutions until they reached 0.5 McFarland standards (approximate cell density = 1.5 × 10^8 cfu/mL) and spectroscopically controlled. The *E. coli* and *S. aureus* strains were inoculated on agar plates. The samples were placed carefully onto agar plates with the aid of sterile forceps, and the agar plates were incubated for 24 h. The inhibition zones around the nAg-loaded TPU wound dressings were compared with those of the TPU mats without silver particles.

Cytotoxicity and Cell Proliferation

The absence of cytotoxic factors is essential for epithelialization, which is facilitated by fibroblasts. Hence, the cell viability on the antibacterial TPU melt-electrospun mats was evaluated

indirectly by tetrazolium salt colorimetric assay (MTT) on the basis of a procedure adapted from the ISO 10993-5 standard test method.

The cytotoxic effect of the unmodified and modified TPU mats on the mouse fibroblast cells was investigated with an indirect cytotoxicity assay. Before sterilization with 70% ethanol for 30 min, the TPU melt-electrospun mats were cut to 0.5 × 0.5 cm^2 samples. They were washed with PBS and cell culture medium. The TPU samples were incubated for 9 days in fresh culture medium to obtain extraction medium at 37°C. All of the fiber mats were removed from the extraction media at the end of the 1st, 3rd, 5th, 7th, and 9th days. The mouse fibroblasts (L929) were cultured in RPMI1640 medium supplemented with 10% fetal bovine serum, 1.0% penicillin–streptomycin, and 1.2% glutamine. The L929 cell line was cultured at 37°C in a 5% CO_2 atmosphere until a confluence in 80% of the flasks occurred. Trypsinized mouse fibroblast cells from the passage of seven cells were counted with a hemocytometer and seeded at a density of 2×10^4 per well onto the TPU fiber mats and cultured overnight in 96-well plates at 37°C. The next day, the culture medium was replaced with extraction medium, and the cells were incubated for 24 h. A volume of 100 μL of MTT solution (5 μg/mL, diluted with RPMI 1640 without phenol red) was added to each well and maintained in the dark for 3 h. A 100 μL/well isopropyl alcohol–HCl solution (absolute isopropyl alcohol containing 0.04*M* HCl) was added to dissolve the insoluble MTT formazan. The plates were read at 570 nm on an ASYS Expert Plus ELISA reader. The cell viability of the control group (plate tissue culture polystyrene) was accepted as 100%, and the relative cell viability was calculated respect to this value and compared with that of the unmodified TPU mats ($n = 8$).

A direct-contact assay was used to determine the mouse fibroblast cell proliferation on the TPU mats over 5 days. Unmodified and modified TPU mats were sterilized with 70% ethanol for 30 min for the cell proliferation test (Length × Width: 0.5 × 0.5 cm^2) and placed in 96-well cell culture plates. The unmodified TPU mat was used as a control in a cell proliferation experiment. L929 mouse fibroblast cells were seeded on the surface of the TPU samples at 2×10^4 cells/well ($n = 3$). The samples were treated with MTT and 0.04*M* HCl in isopropyl alcohol solutions, respectively. The optical density of the solutions was measured at 570-nm wavelengths by an ELISA reader.

The morphology of the fibroblast cells (L929) seeded on the TPU mats was examined by SEM. After sterilization, the cells were seeded on the samples in a 96-well culture plate (4×10^4 cells/well). After 3 days, the samples were fixed with 4% glutaraldehyde solutions for 2 h. The samples were washed with PBS (pH 7.2) and immersed in ethanol solutions (50, 70, 90, and 100% v/v). Finally, the TPU mats were treated with hexamethyldisilazane to dehydrate them and placed into a fume hood to remove the hexamethyldisilazane. The samples were coated with gold/palladium for SEM analysis.

Statistical Analysis

The results are expressed as the mean plus or minus the standard deviation following the expectation-maximization algorithm (EM). The statistical analysis of the water uptake, contact angle, cell proliferation, and indirect cytotoxicity results was performed with PASW Statistics 18 Software (SPSS, Inc.). Statistical comparisons were carried out through analysis of the variance. The differences between the modified and unmodified TPU surfaces were evaluated by a Scheffe's test. A value of $p < 0.05$ was considered to be statistically significant.

RESULTS AND DISCUSSION

Morphology of the Melt-Electrospun TPU Mats

A stable spinning process is feasible by the proper adjustment of the parameters. Hence, TPU was successfully spun with a voltage of 50 kV, a working distance of 6 cm, a temperature of the thermocouple and hot coil of 225–230°C, and a flow rate of 0.1 mL/h.

Figure 2 shows representative SEM images of the melt-electrospun TPU mats. An average diameter of 4.89 ± 0.94 μm was determined. The cross-sectional and surface images demonstrated an interconnected fiber morphology without bead formation. The structure was highly porous and could provide gas exchange for wound healing. Figure 2 shows the diameter distribution histograms of the melt-electrospun TPU. A number of 500 fibers were randomly measured for the determination of this distribution. The TPU fiber diameters ranged from 1 to 7 μm. A total of 70% of the fibers measured had a diameter of 3–4 μm, and the median of total measurements was 3.5 μm. This emphasized the uniform distribution of the fiber diameters.

Thermal and Mechanical Properties of the Melt-Electrospun TPU Mats

The thermal behaviors of the pure PU and melt-electrospun PU mats are illustrated in Figure 3. The pure polymer exhibited two T_m values, one at 123.7°C and the second at 166.8°C. As Zapletalova et al.[22] reported, at 125°C, the endothermic peak was correlated with the dissociation of the hydrogen bonding between the NH groups. The endothermic peak at 170°C exhibited the melting of the PU hard segment. The melt-electrospun samples showed only one T_m. The T_m values of the melt-electrospun mats were 165.9, 169.7, 166.2, and 163.7°C, respectively, for the unmodified TPU mat, PEG-modified TPU mat, and the 0.5 mg/mL and 1 mg/mL nAg loaded TPU mats. After the melt-electrospinning process, a shift in T_m was not observed. The crystallization temperatures of the melt-electrospun PU mat and the modified samples (with PEG and nAg) shifted to a higher temperature compared to that of the pure polymer. In particular, the TPU mat containing 0.5 mg/mL nAg showed a sharper crystallizations peak. The T_g and melt enthalpy ΔH_g values of the samples were 85.27°C and 8.31 J/g for the pure polymer, 87.23°C and 9.48 J/g for the unmodified TPU mat, 87.57°C and 9.53 J/g for the PEG-modified TPU, 87.73°C and 8.44 J/g for the 0.5 mg/mL nAg loaded TPU mat and 87.25°C and 9.36 J/g for the 1 mg/mL nAg loaded TPU mat. An increase in the nAg concentration increased T_g. This was interpreted as the interactions of the nAg's with the molecular structure of the polymer.[23–25]

TGA is frequently used to determine polymer degradation temperatures and absorbed moisture. Figure 4 shows the TGA thermograms of the pure TPU and fiber mats. Slade and Jenkins[26] reported that the weight loss of polyether PU began at 280°C.

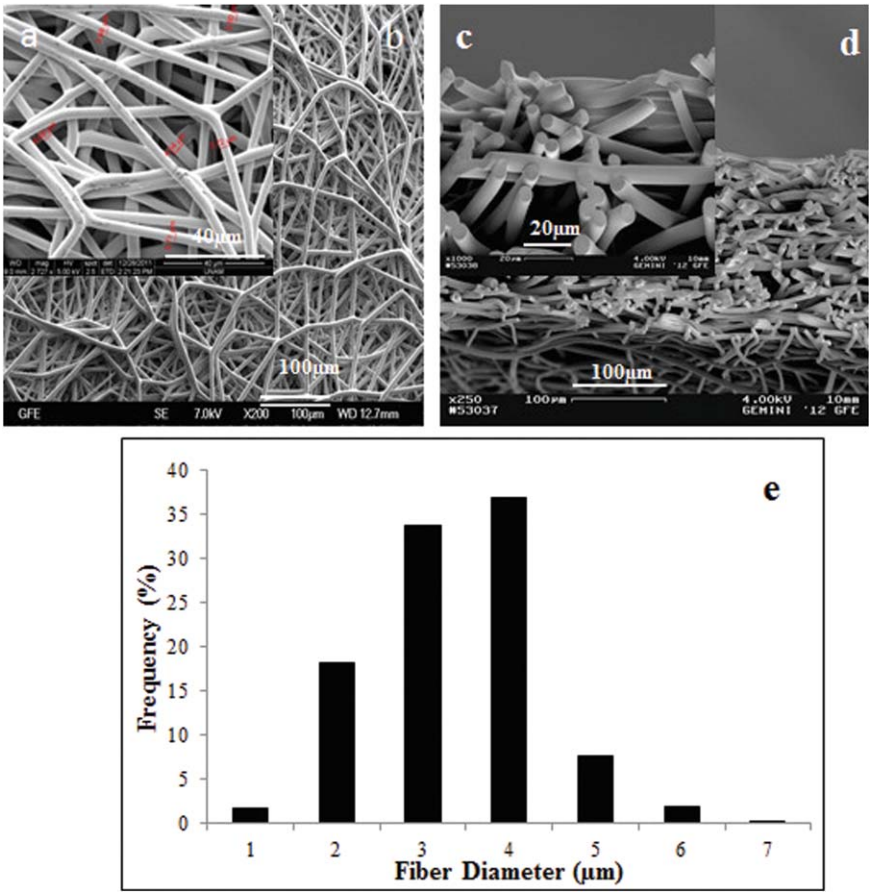

Figure 2. SEM micrographs of the melt-electrospun TPU fibers: (a,b) pure melt-electrospun TPU mats, (c,d) cross-sectional images of TPU mats, and (e) diameter distribution of melt-electrospun TPU mats. An interconnected fiber morphology without bead formation was obtained with an average fiber diameter of 4.89 ± 0.94 μm. [Color figure can be viewed in the online issue, which is available at wileyonlinelibrary.com.]

There was a second decomposition peak at about 325°C, and weight loss occurred at 400°C. This information was in accordance with the TGA diagrams of the pure TPU and TPU mats. The TGA curves showed a loss of mass between 250 and 500°C. The TGA thermograms of the pure PU and melt-electrospun TPU mats indicated no difference. Hence, we concluded that during the melt-electrospinning process, the PU preserved its thermal stability because it was processed at 220–230°C.

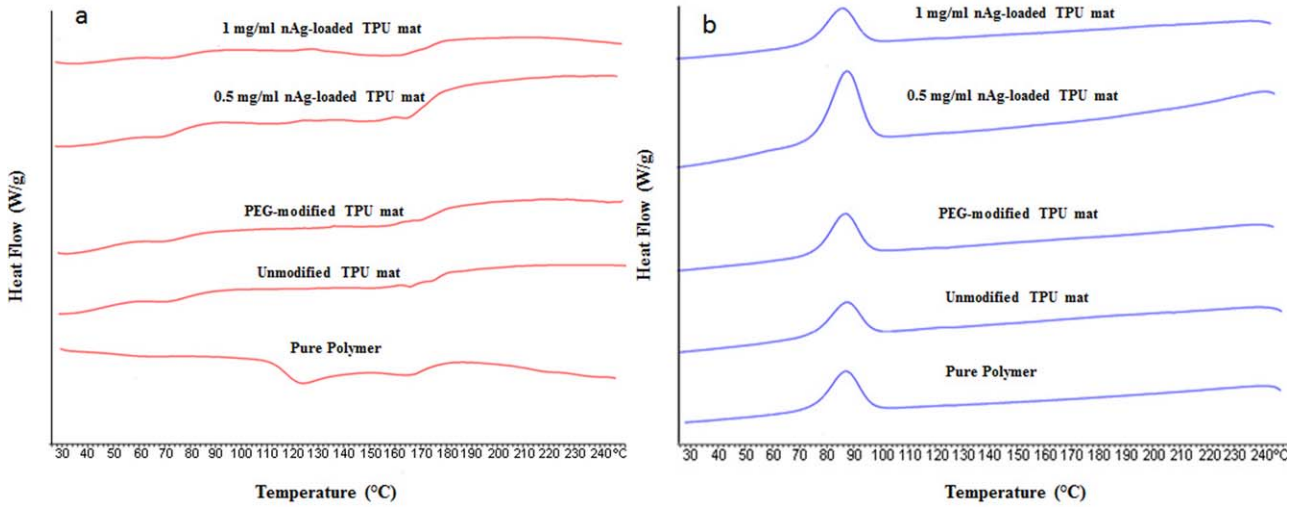

Figure 3. (a) Melting and (b) crystallization behavior of the samples. After melt-electrospinning, a shifting of T_m was not observed. [Color figure can be viewed in the online issue, which is available at wileyonlinelibrary.com.]

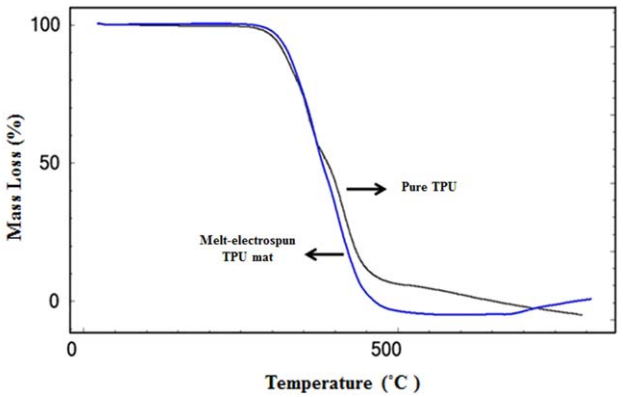

Figure 4. TGA curves of the pure TPU and melt-electrospun TPU mats. TPU mats after the melt-electrospinning process did not show signs of thermal decomposition. [Color figure can be viewed in the online issue, which is available at wileyonlinelibrary.com.]

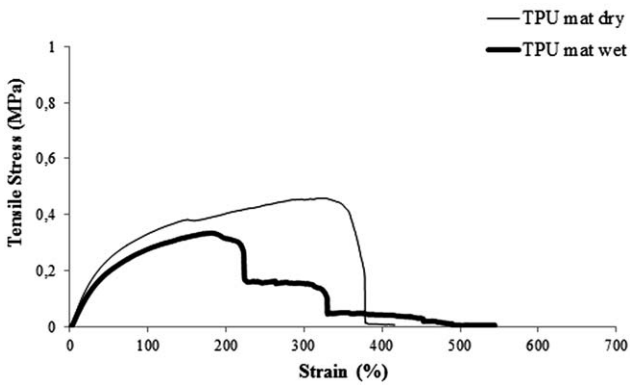

Figure 5. Stress–strain curves of the dry and wet melt-electrospun TPU mats. The tensile strength and elongation were reduced under humid conditions.

The tensile strength and elongation were measured to estimate the mechanical properties of the unmodified TPU mat. To qualitatively compare the effect of humidity, dry and wet samples were tested. The stress–strain curves of the wet and dry melt-electrospun TPU mats are shown in Figure 5. The melt-electrospun dry TPU mat had a tensile strength of 0.4 ± 0.06 MPa and an elongation at break of 390% ± 120.48. The wet TPU mat had a reduced tensile strength of 0.35 ± 0.008 MPa and an elongation at break of 200 ± 22.43%. The tensile strength, elongation, and Young's modulus were relevant data for the assessment of the TPU mats as wound dressings. If a wound-dressing material is elastic, it can fit adequately at the wound site and protect it from external influence.[27] It has been reported that skin simulants showed a tensile strength of 18 ± 2 MPa and an elongation at break of $65 \pm 5\%$.[28] Karchin et al.[20] found that the average ultimate tensile strength and elongation of melt-electrospun TPU were 36.7 ± 9.9 MPa and $221 \pm 95.1\%$. The absolute values of the tensile strength in this study were below the values reported in the aforementioned literature. Because of the smaller size of our samples compared to those in the aforementioned study, the impurities and fiber orientation had a strong effect on the results of the mechanical tests. Additionally, the mean fiber diameter of our samples was smaller. We must emphasize here that a quantitative comparison could be conducted if the size of the samples were synchronized. This procedure would be particularly interesting for evaluating the optimal synthesis route for the polymer and the effect of the plasma treatment and functionalization on the mechanical properties of TPU mats and scaffolds in the future.

Surface Modifications

The color of the melt-electrospun TPU mats changed from white to yellow–brown after UV irradiation because of the reduction of Ag^+ ions into elemental Ag (i.e., nAg). This color change indicated Ag nanoparticle situated on the surface of the electrospun TPU mat. SEM images of the melt-electrospun TPU fibers containing nAg's are shown in Figure 6. These images demonstrate qualitatively that the nAg's were situated after UV irradiation on the fiber surface and were distributed homogeneously. Additionally, the appearance of the adsorbed nAg's on the surface increased with the silver concentration.

The effect of the surface modifications on the surface chemical composition was determined by XPS measurements. The binding energy values of C_{1s}, N_{1s}, and O_{1s} of the unmodified TPU mat were 285.98, 400.5, and 532.14 eV, respectively. The C_{1s}, N_{1s}, and O_{1s} peaks of the unmodified TPU mats were as reported in literature.[29,30] The XPS atomicity percentages of the

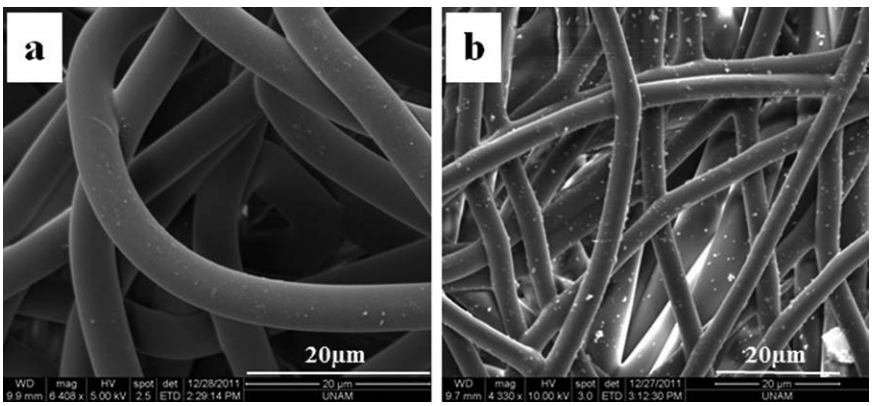

Figure 6. SEM micrographs of the melt-electrospun TPU mats containing (a) 0.5 and (b) 1 mg/mL nAg. A distribution of nAg's on the TPU fiber surface after UV irradiation was observed.

Table I. Surface Elemental Compositions and Proportions on the TPU Mats

	Atomic concentration (%)				
	C	O	N	Ag	O/C
Unmodified melt-electrospun TPU mat	79.22	17.96	2.82	—	0.22
PEG-modified melt-electrospun TPU mat	76.08	18.58	3.18	—	0.24
0.5 mg/mL nAg loaded melt-electrospun TPU mat	67.22	21.69	4.93	3.15	0.32
1 mg/mL nAg loaded melt-electrospun TPU mat	71.84	20.47	4.39	3.3	0.28

The XPS results demonstrated the application of nAg's due to the functionalization process.

TPU melt-electrospun mats are summarized in Table I. After PEG–plasma modifications, the ratio of oxygen to carbon (O/C) increased as a result of the generated hydroxyl group on the TPU mat surface. The maximum peak of nitrogen shifted to 400.3 from 400.5 eV after plasma treatment. This behavior could be explained as the new bond formation on the melt-electrospun TPU surface by dissociation of the N—H bond.[31]

After the adsorption of nAg's on the PEG-modified TPU melt-electrospun mat, the intensities of the C_{1s}, O_{1s}, and N_{1s} peaks decreased at both silver concentrations. This behavior might have been due to the formation of Ag—O or Ag—N bonds.[32] The elemental percentage of Ag_{3d} increased with the silver concentration. The valence-band spectra of the nAg's (Ag_{3d}) at various concentrations (0.5 and 1 mg/mL) were obtained at 368.43 and 368.17 eV, respectively. We concluded from these results that the application of PEG and silver on the surface was successful.

Contact Angle and Water Uptake of the Melt-Electrospun TPU Mats

The contact angle of the PU melt-electrospun mat was around $114 \pm 2.8°$; this was in agreement with the hydrophobicity of the pure polymer. Additionally, no statistically significant difference was observed between the contact angle values of the pure and functionalized melt-electrospun TPU mats. The 0.5 and 1 mg/mL nAg loaded TPU mats had contact angle values of 117 ± 0.04 and $113.8 \pm 0.08°$, respectively. Although the PEG-modified TPU mats ($110 \pm 0.4°$) indicated a slight decrease of 4° because of its hydrophilic properties, all of the samples showed similar behavior in response to direct contact with water before and after modification. However, we observed during the trials that the contact angle of water sessile drops on the melt-electrospun TPU mats tended to decrease with contact time. To assess the wettability and water absorption over a longer period of time, the water uptake was tested.

Water-uptake tests were performed for 1 and 24 h. As shown in Figure 7, the water uptake of the PEG-modified TPU mat was higher compared to that of the unmodified TPU mat at the end of 1 h ($p < 0.005$). PEG modification enhanced the water absorption behavior of the melt-electrospun TPU mats. The obtained result was confirmed by studies in the literature.[30] The water absorbability of the nAg-containing TPU melt-electrospun mat increased over time and reached 200% at the end of 24 h. As previous researchers reported, the water-uptake behavior of the structure was influenced by the nAg-access on the surface.[25,30] This behavior could be explained by the superficial energy of the nAg's. nAg's in the solution could interact with the oxygen atoms, combine with hydrogen atoms, and generate hydrogen bonds.[32] Interestingly, the TPU melt-electrospun mats could reach a water absorbability of more than 100% of the initial weight, whereas typical film dressings usually take up 2 to 3% of the initial weight.[33] This effect was attributed to the porous properties due to the open fibrous structure of the mats. Therefore, the water-uptake test results showed that the melt-electrospun TPU mats had suitable hydrophilic properties after modification, for example, to manage wound exudate.

Silver Release of the Melt-Electrospun TPU Mats

The silver-release properties of an antibacterial wound dressing are important with respect to its wound-healing performance. Wound dressings should provide a prolonged and uniform silver release during application. The silver-ion-release rate from the melt-electrospun mats were obtained by ICP-MS and are shown in Figure 8. Samples with 1 mg/mL nAg showed a burst-like release profile in the first day compared to samples with 0.5 mg/mL nAg. This burst release behavior could be explained as a result of the rapid water uptake within the first 24 h.[34] Hence, the silver-ion release increased with the increasing water content of the polymer. Alternatively, the burst behavior could be explained by the concentration gradient between the fibrous

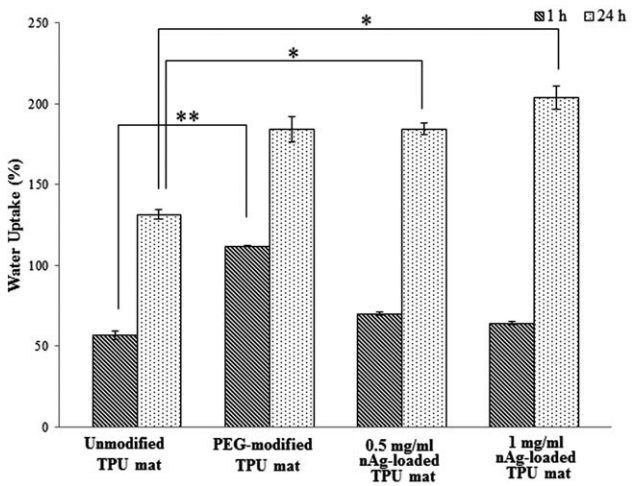

Figure 7. Water uptake of the melt-electrospun TPU mats. Water uptake was increased by surface modification. The values are presented as means plus or minus expectation-maximization algorithm (EM) ($n = 3$, $^*p < 0.05$ and $^{**}p < 0.005$ in comparison with an unmodified TPU mat).

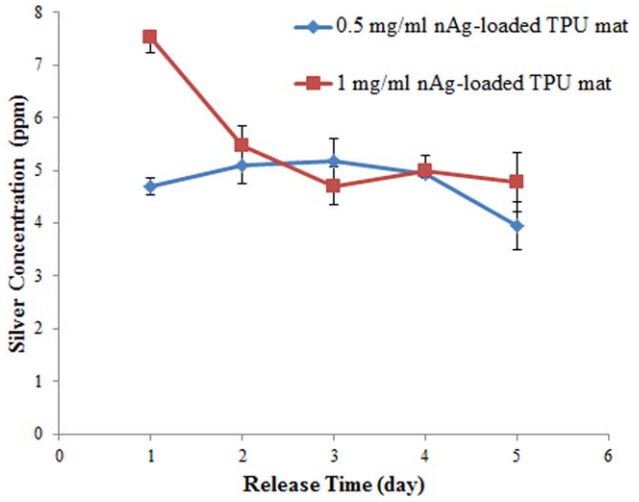

Figure 8. Silver-release properties of the 0.5 and 1 mg/mL nAg loaded TPU mats. Both of the nAg-loaded TPU mats uniformly released silver over 4 days. The values are presented as means plus or minus EM ($n = 3$). [Color figure can be viewed in the online issue, which is available at wileyonlinelibrary.com.]

mat and its environment. The concentration gradient is the driving force for diffusion, and its value depends on the difference between the concentrations of silver on the fiber surface and in the surrounding environment. Taking the SEM images into account (Figure 6), we attributed this burst-diffusion-related burst behavior to the increased number of silver particles on the fiber surface for the 1 mg/mL nAg mats.

ICP-MS measurements demonstrated that apart from the initial burst release for the higher nAg loading, the modified TPU mats released silver constantly over a period of up to 4 days. Commercial wound-dressing products provide controlled release for between 3 and 7 days.[35] With respect to the silver-release properties, the modified TPU mats were capable of competing with commercial products.

Antibacterial Study of the TPU Melt-Electrospun Mats

In the case of a wound infection, the required nutrients and oxygen for wound healing are consumed by bacteria and fungi. Then, the amount of growth factors and cytokines, which stimulate wound healing, decreases. This situation might lead to tissue death. Therefore, the functionalization of wound-dressing materials with antibacterial activity is important for the healing process.[35]

The antibacterial activity results of the melt-electrospun TPU mats are shown in Figure 9. The unmodified and PEG-modified TPU melt-electrospun mats had no antibacterial properties; therefore, no dark zone was observed around the unmodified and PEG-modified melt-electrospun TPU discs. The antibacterial response was observed for both silver concentrations. The 1 mg/mL nAg loaded TPU melt-electrospun mats produced a larger zone of inhibition against both bacteria species compared to the 0.5 mg/mL nAg loaded mat. The *E. coli* inhibition zone

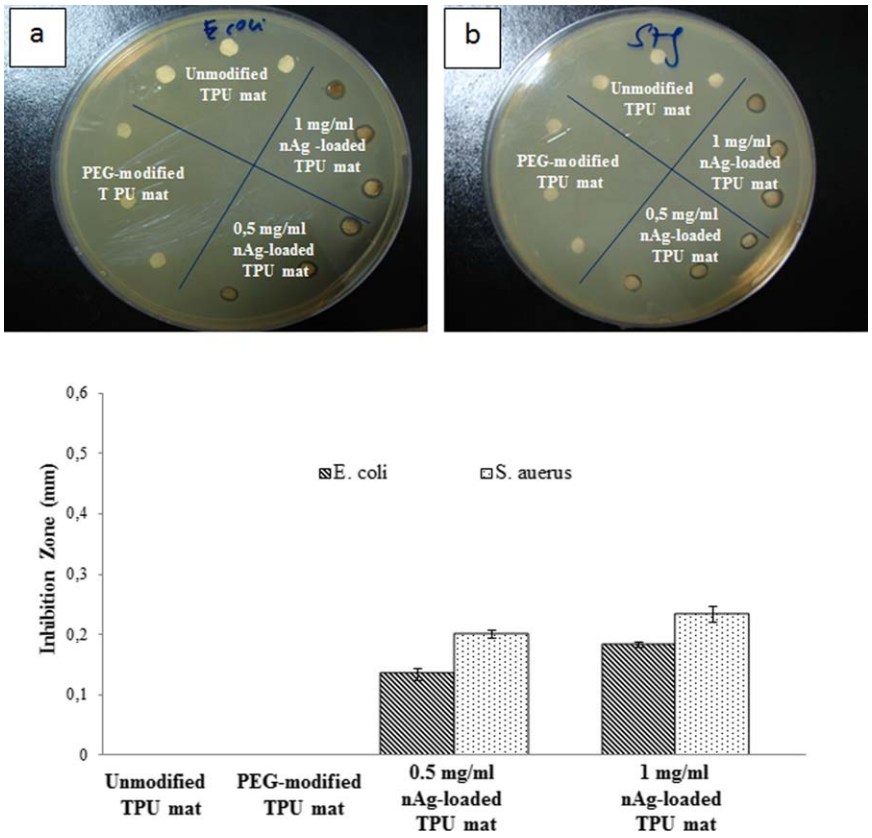

Figure 9. Inhibition zones around the TPU mats after 12 h for two different bacteria: (a) *S. aureus* and (b) *E. coli*. Antibacterial activity is observed due to silver modification. [Color figure can be viewed in the online issue, which is available at www.interscience.wiley.com.]

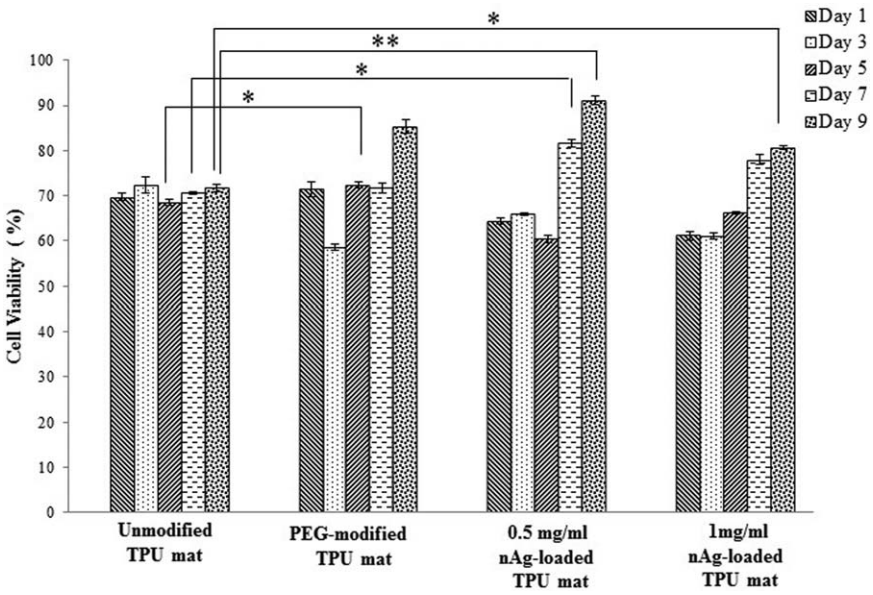

Figure 10. Relative cell viability on the TPU melt-electrospun mats. The 0.5 and 1 mg/mL nAg loaded TPU mats showed higher cell viability than the unmodified TPU mat on the 7th and 9th days. The values are presented as means plus or minus EM ($n = 8$, $^{*}p < 0.05$ and $^{**}p < 0.005$ in comparison with the unmodified TPU mat).

values of the 0.5 and 1 mg/mL nAg loaded TPU mats were 0.13 ± 0.015 and 0.18 ± 0.002 mm, respectively. The *S. aureus* inhibition zone values of the 0.5 and 1 mg/mL nAg loaded TPU mats were 0.20 ± 0.01 and 0.25 ± 0.02 mm, respectively. The antibacterial activity increased with higher silver concentration.[36]

Park et al.[37] reported that a PEG-modified PU surface reduces bacterial adhesion. The 0.5 and 1 mg/mL nAg loaded melt-electrospun TPU mats showed increased antibacterial performance against *S. aureus* in comparison to *E. coli*. This result suggests that nAg's on the PEG-modified surface penetrated into the cell wall, although the Gram-positive bacteria (*S. aureus*) had a thicker outer peptidoglycan multilayer than the Gram-negative bacteria (*E. coli*) with their inner single layer. Albeit the differences in respect to the bacteria types, the antibacterial assays/disc-diffusion method in connection with the ICP-MS trials indicated that a loading of 0.5 mL/mg nAg was sufficient for an antibacterial wound dressing with stable release properties over a period of 4 days.

In Vitro Evaluation of the TPU Melt-Electrospun Mats

The metabolic activity of the cells was assessed with MTT assays. Figure 10 demonstrates the effect of each modification on the fibroblasts. The unmodified melt-electrospun TPU mat showed no significant change in the cell viability values during the cell activity tests. The PEG-modified TPU melt-electrospun mat presented a higher cell viability compared to the unmodified counterparts at the end of 5 days ($p < 0.05$). This underlined a study reported in the literature, in which PEG modification increased the cell adhesion, spreading, and proliferation.[38] Additionally, the response of the nAg-loaded PEG-modified TPU mat was investigated in terms of its silver cytotoxicity. Poon and coworkers[39,40] reported that silver is highly toxic to fibroblasts and keratinocytes. There are also reports in literature that directly correlate the cell toxicity with the silver concentration.[41] Braydich-Stolle et al.[42] investigated the issue, and concentrations of nAg's between 5 and 10 mg/mL induced necrosis or apoptosis of mouse spermatogonial stem cells. In this study, significantly lower concentrations of nAg's were applied for the TPU surface modification. TPU mats with 0.5 and 1 mg/mL nAg seemed to result in high percentages of viable cells on the 7th and 9th days compared to the unmodified TPU mat ($p < 0.05$).

Cell proliferation on the melt-electrospun TPU mat seemed to increase for all of the investigated samples over the course of 5 days (Figure 11). The cell number on the PEG-modified melt-electrospun TPU mat compared to that of the unmodified group increased significantly at the end of the 5th day in the cell proliferation test, as expected ($p < 0.05$). The silver-loaded TPU mats demonstrated a lower cell proliferation rate compared to the PEG-modified TPU mats. However, they reached the formazan absorbance of the unmodified TPU mat at the end of 5 days. Hence, we concluded that cell proliferation was not significantly hindered by silver addition.

The morphology of the cultured cells on the TPU mats was investigated by SEM. SEM images were obtained after 3 days of incubation. In correlation with the viability and proliferation tests, it is shown in Figure 12 that the fibroblasts adhered on and infiltrated into the unmodified and modified melt-electrospun TPU mats. The observed cell morphologies on the 0.5 and 1 mg/mL nAg loaded melt electrospun mats were not different from those of the unmodified mats. This indicated that there seemed to be no effect of cytotoxicity because of the materials used in this study after 3 days of incubation. Hence, we expect that the surface modification would have no negative effect on the process of wound healing (e.g., epithelialization).

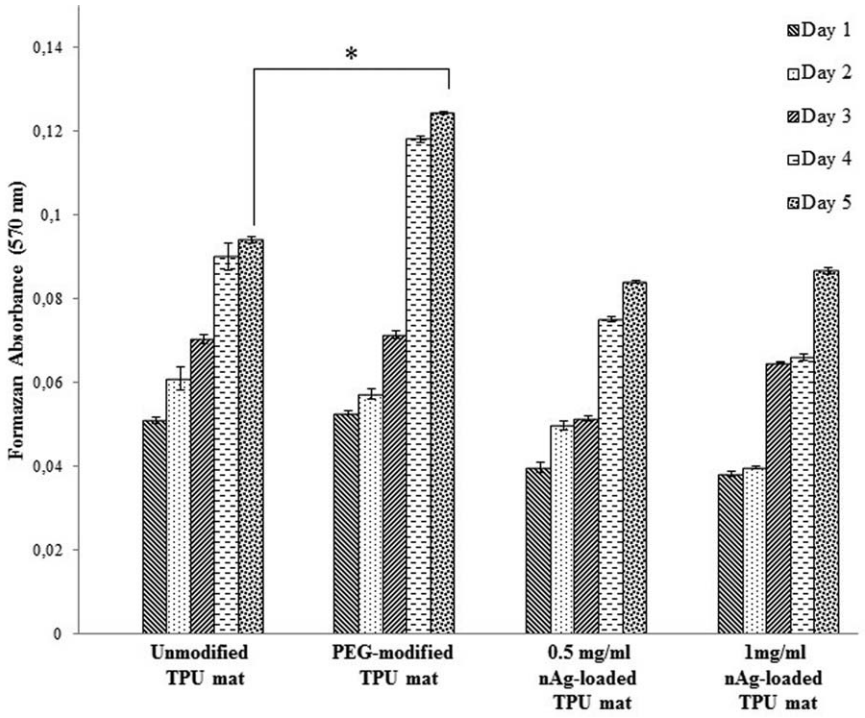

Figure 11. Cell proliferation on the TPU melt-electrospun mats. The cell number increased on the PEG-modified, melt-electrospun TPU mat in comparison with the unmodified group at the end of the 5th day. The values are presented as means plus or minus EM ($n = 3$, $^*p < 0.05$ in comparison with the unmodified TPU mat).

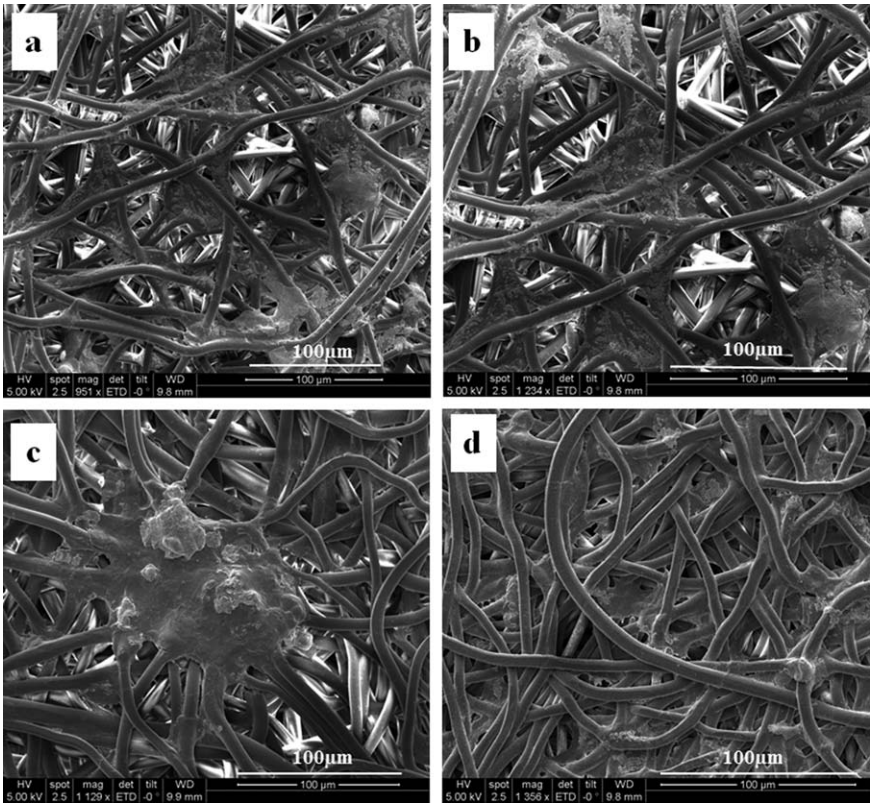

Figure 12. SEM images of fibroblasts (L929) cultured (a) on the unmodified TPU melt-electrospun TPU mat, (b) on the PEG-modified TPU mat, (c) on the 0.5 mg/mL nAg loaded TPU mat, and (d) on the 1 mg/mL nAg loaded TPU mat. After 3 days of incubation, cell adhesion and spreading were observed for all four materials.

CONCLUSIONS

The aim of this study to demonstrate a feasible processing for producing porous wound dressings with antibacterial modification was successful. Fibrous TPU mats with an average uniform fiber diameter of 4.89 ± 0.94 μm were prepared by a melt-electrospinning process. The surfaces of the melt-electrospun TPU mats were modified with nAg's and PEG to enhance the antibacterial and water-uptake properties without cytotoxic side effects. The processability was underlined by the thermal analysis of the TPU, which demonstrated that no thermal decomposition occurred during the spinning process.

ICP-MS measurements demonstrated that apart from an initial burst release for the higher nAg loading, the modified TPU mats released silver constantly over a period of up to 4 days. In connection with the antibacterial assays/disc-diffusion method, which indicated an inhibition zone for both concentrations, we suggest that a loading of 0.5 mL/mg nAg is sufficient for an antibacterial wound dressing with stable release properties. Contact angle measurements indicate that the instant wettability of the nonwoven mats was independent of the surface modification. In connection with the water-uptake measurements, we presumed that the surface modification increased the ability to store water within the nonwoven structure over a longer period of time (e.g., 1 and 24 h). This could be an important feature for a wound dressing with humidity-managing properties that takes up excess wound exudate and stores it inside. Additionally, the surface modification had no cytotoxic effect on the fibroblast over the course of 3 days. This is a valuable property for the wound-healing process.

Preliminary studies of the mechanical properties (e.g., tensile strength, elongation) qualitatively showed reduced values of wet samples in comparison to those of dry specimens. Moreover, the values were below the values reported in the literature. However, these values cannot be used for benchmarking with other studies because the morphology and size of the tested specimens differed from those in other studies. We suggest that a quantitative comparison be conducted with samples of equivalent size and structure. This procedure would be particularly interesting for evaluating the optimal synthesis route for the polymer and the effect of posttreatment on the mechanical properties of the TPU mats and scaffolds in the future.

Additionally, the results of this investigation highlight procedures for further studies, in which the modified melt-electrospun TPU mats could be compared to commercial wound-dressing materials.

ACKNOWLEDGMENTS

The authors are grateful to Tayfun Vural and Murat Demirbilek (Hacettepe University) for their considerable assistance with the analytical methods. Additionally, the authors thank Kai Bruening (BASF S.E., Lemfoerde, Germany) for providing TPU samples for the experimental trials.

REFERENCES

1. Quinn, K. J.; Courtney, J. M.; Evans, J. H.; Gaylor, J. D. S. *Biomaterials* **1985**, *6*, 369.
2. Zahedi, P.; Rezaeiana, I.; Ranaei-Siadat, S.; Jafaria, S.; Supaphol, P. *Polym. Adv. Technol.* **2010**, *21*, 77.
3. Bergeron, M.; Levesque, S.; Guidion, R. G. In Biomedical Applications of Polyurethanes; Vermette, P., Griesser, H. J., Laroche, G., Guidoin, R., Eds.; Landes Bioscience: Georgetown, TX, **2001**; p 220.
4. Broekema, F. I.; Oeveren, W.; Zuidema, J.; Visscher, S. H.; Bos, R. R. M. *Mater. Sci.: Mater. Med.* **2011**, *22*, 1081.
5. Khil, M.; Cha, D.; Kim, H.; Kim, I.; Bhattarai, N. *Appl. Biomater.* **2003**, *67*, 675.
6. Pavlova, M.; Draganova, M. *Biomaterials* **1993**, *14*, 13.
7. Lelah, M. D.; Cooper, S. L. Polyurethanes in Medicine; *CRC: Boca Raton, FL*, **1986**; p 23.
8. Hilton, J. R.; Williams, D. T.; Beuker, B.; Miller, D. R.; Harding, K. G. *Clin. Infect. Dis.* **2004**, *39*, S100.
9. Klasen, H. *Burns* **2000**, *26*, 117.
10. Lansdown, A. B. *J. Wound Care* **2002**, *11*, 125.
11. Wright, J. B.; Lam, K.; Burrell, R. E. *Am. J. Infect. Control* **1998**, *26*, 572.
12. Percival, S. L.; Thomas, J. G.; Slone, W.; Linton, S.; Corum, L.; Okel, T. *Wound Repair Regen.* **2011**, *19*, 767.
13. Ip, M.; Lui, S. L.; Poon, V. K. M.; Lung, I.; Burd, A. *J. Med. Microbiol.* **2006**, *55*, 59.
14. Atiyeh, B. S.; Costagliola, M.; Hayek, S. N.; Dibo, S. *Burns* **2007**, *33*, 139.
15. Tian, J.; Wong, K. K. Y.; Ho, C.; Lok, C.; Yu, W.; Che, C.; Chiu, J.; Tam, P. K. H. *Chem. Med. Chem.* **2007**, *2*, 129.
16. Ramakrishna, S.; Fujihara, K.; Teo, W.-E.; Lim, T. C.; Ma, Z. An Introduction to Electrospinning and Nanofibers; *World Scientific: Singapore*, **2005**; p 22.
17. Huang, Z. M.; Zhang, Y. Z.; Kotaki, M.; Ramakrishna, S. *Compos. Sci.* **2003**, *63*, 2223.
18. Reneker, D. H.; Yarın, A. L.; Zussman, E.; Xu, H. *Adv. Appl. Mech.* **2007**, *41*, 43.
19. Hutmacher, D. W.; Dalton, P. D. *Chem. Asian J.* **2010**, *6*, 44.
20. Karchin, A.; Simonovsky, F. I.; Ratner, B. D.; Sanders, J. E. *Acta Biomater.* **2011**, *7*, 3277.
21. Dalton, P. D.; Calvet, J. L.; Mourran, A.; Klee, D.; Möller, M. *Biotechnol. J.* **2006**, *1*, 998.
22. Zapletalova, T.; Michielsen, S.; Pourdeyhimi, B. *J Eng. Fiber Fabrics* **2006**, *1*, 62.
23. Kumar, R.; Münstedt, H. *Polym. Int.* **2005**, *54*, 1180.
24. Shi, Q.; Vitchuli, N.; Nowak, J.; Noar, J.; Caldwell, J. M.; Breidt, F.; Bourham, M.; McCord, M.; Zhang, X. *J. Mater. Chem.* **2011**, *21*, 10330.
25. Lakshman, L.; Shalumon, K. T.; Nair, S.; Jayakumar, R.; Nair, S. V. *J. Macromol. Sci. Pure Appl. Chem.* **2010**, *47*, 1012.
26. Slade, P. E., Jr.; Jenkins, L. T. *J. Polym. Sci. Part C: Polym. Symp.* **1964**, *6*, 27.
27. Waring, M.; Biefeldt, S.; Matzold, K. P.; Butcher, M. *J. Wound Care* **2011**, *20*, 412.
28. Jussila, J.; Leppaeniemi, A.; Paronen, M.; Kulomaekim, E. *Forensic Sci. Int.* **2005**, *150*, 63.

29. Weibel, D. E.; Vilani, C.; Habert, A. C.; Achete, C. A. *J. Membr. Sci.* **2007**, *293*, 124.

30. Chen, J.; Chiang, Y. *J. Nanosci. Nanotechnol.* **2010**, *10*, 7560.

31. Serghini-Monim, S.; Norton, P. R.; Puddephatt, R. J. *J. Phys. Chem. B* **1997**, *101*, 7808.

32. An, J.; Zhang, H.; Zhang, J.; Zhao, Y.; Yuan, X. *Colloid Polym. Sci.* **2009**, *287*, 1425.

33. Dabney, S. E. *Ph.D. Thesis, University of Akron*, **2002**.

34. Kumar, R.; Munstedt, H. M. *Biomaterials* **2005**, *26*, 2081.

35. Fong, J.; Wood, F. *Int. J. Nanomed.* **2006**, *1*, 441.

36. Ma, Z.; Ji, H.; Tan, D.; Teng, Y.; Dong, G.; Zhou, J.; Qiu, J.; Zhang, M. *Colloids Surf. A* **2011**, *387*, 57.

37. Park, K. D.; Kim, Y. S.; Han, D. K.; Kim, Y. H.; Lee, E. H.; Suh, H.; Choi, K. S. *Biomaterials* **1998**, *19*, 851.

38. Demirbilek, M. E.; Demirbilek, M.; Karahaliloğlu, Z.; Erdal, E.; Vural, T.; Yalçın, E.; Sağlam, N.; Denkbaş, E. B. *Appl. Biochem. Biotechnol.* **2011**, *164*, 780.

39. Poon, V. K. M.; Burd, A. *Burns* **2004**, *30*, 140.

40. Burd, A.; Kwok, C. H.; Hung, S. C.; Chan, H. S.; Gu, H.; Lam, W. K.; Huang, L. *Wound Repair Regen.* **2007**, *15*, 94.

41. Ziegler, K.; Gorl, R.; Effing, J.; Ellermann, J.; Mappes, M.; Otten, S.; Kapp, H.; Zoellner, P.; Spaeth, D.; Smola, H. *Skin Pharmacol. Physiol.* **2006**, *19*, 140.

42. Braydich-Stolle, L.; Hussain, S.; Sclager, J. J.; Hofmann, M. C. *Toxicol. Sci.* **2005**, *88*, 412.